

## Method for Evaluating Reliance Level of a Virtual Metrology System<sup>1</sup>

Fan-Tien Cheng<sup>2\*</sup>, *Senior Member, IEEE*, Yeh-Tung Chen\*, *Student Member, IEEE*,  
Yu-Chuan Su\*\*, *Member, IEEE*, and Deng-Lin Zeng\*

\*Institute of Manufacturing Engineering  
National Cheng Kung University  
Tainan, Taiwan, R.O.C.

\*\*Department of Computer Science & Information Engineering  
Far East University  
Tainan, Taiwan, R.O.C.

**Abstract** - A method for evaluating reliance level of a virtual metrology system (VMS) is proposed. This method calculates a reliance index (*RI*) value between 0 and 1 by analyzing the process data of production equipment to decide if the virtual metrology result is reliable. A *RI* threshold is also defined in this method. If a *RI* value is higher than the threshold, the conjecture result is reliant; otherwise, the conjecture result needs to be further examined. In addition to the *RI*, the method also proposes process data similarity indexes (*SI*s). The *SI*s are defined to evaluate the degree of similarity between the input set of process data and those historical sets of process data used to establish the conjecture model. Two kinds of *SI*s are included in the method: global similarity index (*GSI*) and individual similarity index (*ISI*). Both the *GSI* and *ISI* are applied to assist the *RI* in gauging the reliance level and locating the key parameter(s) that cause major deviation, hence the VMS manufacturability problem is resolved. An illustrative example with 300-mm semiconductor foundry production equipment in Taiwan is demonstrated in this work. The real experimental results show that this method is applicable to the VMS of (such as semiconductor and TFT-LCD) production equipment.

**Index Terms** – Reliance level, reliance index (*RI*), degree of similarity, global similarity index (*GSI*), individual similarity index (*ISI*), virtual metrology, manufacturability.

### I. INTRODUCTION

Currently, in most of the semiconductor and TFT-LCD plants, quality of products manufactured from production equipment is monitored by sample-testing, i.e. the products in manufacturing process are selectively tested periodically, or dummy materials (such as monitoring wafers or glass) are actually applied in a manufacturing process and tested so as to monitor whether the quality of the process is acceptable. The conventional method generally assumes that abnormal conditions regarding process quality of production equipment do not occur abruptly, so that measurement results of the selected products or the dummy materials can be used to infer the product quality within a period of production. However, the conventional monitoring method can merely know the quality of the selected products or the dummy materials actually tested, and cannot know the quality of the process in-between the selected products. If abnormal conditions of the production equipment occur between two selected tests, the conventional monitoring

method cannot find out the abnormal conditions in time, thus inferior products may be produced.

For resolving the aforementioned problem, every product should be tested comprehensively. However, testing every product needs to install large amounts of metrology equipment and requires a lot of cycle time. Large amounts of dummy materials will also be wasted. Therefore, it is desired to provide a method, denoted virtual metrology [1], for monitoring process quality without actual measurement, such that quality of production process can be seamlessly monitored in time. Moreover, virtual metrology is essential for wafer-to-wafer advanced process control [1].

When a virtual metrology system (VMS) is used to conjecture a virtual measurement value of a product, if the product happens to be a selected test sample that has an actual measurement value, then the conjecture error of the virtual measurement value can be evaluated. However, in most cases, the product is not a selected test sample, such that no actual measurement value can be provided for comparison with the virtual measurement value. Thus, the accuracy of the virtual measurement value is unknown. A user, consequently, cannot appreciate in time what the reliance level of the virtual measurement value is, such that hesitation about application occurs. This will cause the so-called applicability or manufacturability problem of a VMS [9].

The proposed method has two aspects. One is to define a reliance index (*RI*) for evaluating reliance level of a VMS conjecture result. The other is to formulate process data similarity indexes (*SI*s), including global similarity index (*GSI*) and individual similarity index (*ISI*), for assessing degree of similarity between the input set of process data and the historical sets of process data used for establishing the conjecture model. The purpose of applying the *GSI* and *ISI* to gauge the similarity level is to assist the *RI* in consolidating VMS reliance level and locating the key parameter(s) that cause major deviation.

In accordance with the aforementioned aspects, the method proposed is divided into a training phase, a tuning phase, and a conjecturing phase. The VMS of production equipment in a 300-mm semiconductor foundry in Taiwan was selected as an illustrative example to verify the practicality and manufacturability of the proposed method.

The rest of this work is organized as follows. Section 2 elucidates the algorithms of the *RI*, *GSI*, and *ISI*. Section 3 explains the VMS operating procedures by applying the *RI* and *GSI*. Section 4 elaborates the applicability and

1. The authors would like to thank the National Science Council of the Republic of China for financially supporting this research under contract No: NSC95-2622-E-006-002. This work is Taiwan R.O.C. (App. No. 95116617) and U.S.A. (App. No. 11/617,957) Patent Pending.  
2. The corresponding author (e-mail: chengft@mail.ncku.edu.tw).

implications of the *RI* and *GSI*. Section 5 presents the illustrative example. Finally, Section 6 makes a summary and conclusions.

## II. RI AND SI ALGORITHMS

A block diagram of the VMS possessing the *RI*, *GSI*, and *ISI* is shown in Fig. 1. As depicted in Fig. 1, a data preprocess module processes and standardizes raw process data from a piece of production equipment, and sifts important parameters from all of the original parameters to prevent immaterial parameters from affecting the prediction accuracy [8]. A conjecture model uses a set of input process data after preprocess to conjecture the virtual measurement value. The conjecture algorithm applicable to the conjecture model can be such as a neural-network (NN) algorithm, a multi-regression (MR) algorithm, or a time-series algorithm, etc. When a NN algorithm is adopted, during the training phase, a self-searching means is used to self-search the optimal combination of parameters of the conjecture model [2][3]. A *RI* module generates the *RI* value to estimate the reliance level of the virtual measurement value. A similarity index (*SI*) module calculates the *GSI* and *ISI* values for evaluating the degree of similarity of the input-set process data.

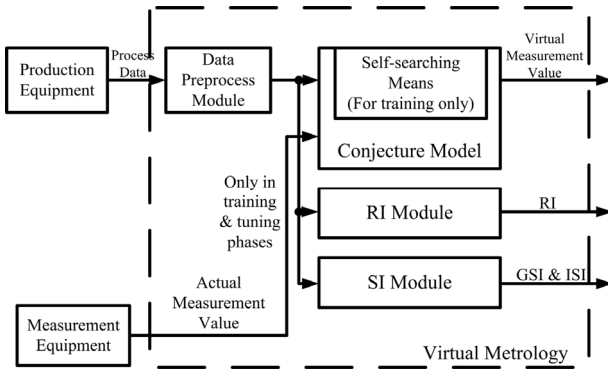


Fig. 1. Block Diagram of a Virtual Metrology System.

The *RI* value is defined to be between 0 and 1. To distinguish how good the *RI* is, an approach for calculating the *RI* threshold value ( $RI_T$ ) is also proposed. If the *RI* is greater than the  $RI_T$ , then the virtual measurement is reliable; otherwise, the reliance level of the virtual measurement is relatively low such that the conjecture result needs further verification.

The definition of the *GSI* is the degree of similarity between the set of process data currently inputted and all of the historical sets of process data in the conjecture model for training and tuning purposes. And, the definition of the *ISI* of an individual process parameter is the degree of similarity between this individual process-parameter's standardized process datum of the input set and the same process-parameter's standardized process data in all of the historical sets for training and tuning the conjecture model. The *GSI* and *ISI* values are utilized to assist the *RI* in gauging the reliance level and identify the key process parameters that cause major deviation.

The operating procedures of the VMS are divided into a training phase, a tuning phase, and a conjecturing phase. In

the following, the algorithms related to the *RI*, *GSI*, and *ISI* are first presented, and then their overall operating procedures are explained.

### 2.1 Reliance Index (RI)

It is assumed that  $n$  sets of historical data are collected, including process data ( $X_i, i = 1, 2, \dots, n$ ) and the corresponding actual measurement values ( $y_i, i = 1, 2, \dots, n$ ), where each set of process data contains  $p$  individual parameters (from parameter 1 to parameter  $p$ ), i.e.  $X_i = [x_{i,1}, x_{i,2}, \dots, x_{i,p}]^T$ . Besides,  $(m-n)$  sets of process data in actual production are also collected, but except  $y_{n+1}$ , no actual measurement values are available. In other words, only the first piece among  $(m-n)$  pieces of the products is selected and actually measured. In the current manufacturing practice, the actual measurement value  $y_{n+1}$  obtained is used for inferring and evaluating the quality of the  $(m-n-1)$  pieces of the products.

In general, a set of actual measurement values ( $y_i, i = 1, 2, \dots, n$ ) is a normal distribution with mean  $\mu$  and standard deviation  $\sigma$ , i.e.  $y_i \sim N(\mu, \sigma^2)$ . All the actual measurement values can be standardized with respect to the mean and standard deviation of the sample set ( $y_i, i = 1, 2, \dots, n$ ). Consequently, their standardized values (also called z scores)  $Z_{y_1}, Z_{y_2}, \dots, Z_{y_n}$  are obtained, where each z score has a mean of zero and a standard deviation of one, i.e.  $Z_{y_i} \sim N(0, 1)$  [4]. With respect to the actual measurement data, when its corresponding  $Z_{y_i}$  is close to 0, it means that the actual measurement value approaches to the central value of the specification. The equations of standardization are listed as follows [4]:

$$Z_{y_i} = \frac{y_i - \bar{y}}{\sigma_y}, \quad i = 1, 2, \dots, n \quad (1)$$

$$\bar{y} = \frac{1}{n} (y_1 + y_2 + \dots + y_n) \quad (2)$$

$$\sigma_y = \sqrt{\frac{1}{n-1} [(y_1 - \bar{y})^2 + (y_2 - \bar{y})^2 + \dots + (y_n - \bar{y})^2]} \quad (3)$$

where  $y_i$  is the  $i$ -th actual measurement value,  
 $Z_{y_i}$  is the standardized  $i$ -th actual measurement value,  
 $\bar{y}$  is the mean of all the actual measurement values, and  
 $\sigma_y$  is the standard deviation of all the actual measurement values.

This work adopts a neural-network (NN) algorithm as the conjecture algorithm for establishing the VMS conjecture model [2][3][7], and uses a multi-regression (MR) algorithm [4] to be the reference algorithm for establishing the reference model that serves as a comparison base of the conjecture model. However, other prediction-oriented algorithms may also be applied to be the conjecture

algorithm or the reference algorithm of the proposed method, as long as the reference algorithm is different from the conjecture algorithm.

When the NN algorithm and the MR algorithm are utilized, if their convergence conditions both are that SSE (Sum of Square Error) is minimum with  $n \rightarrow \infty$ , their standardized predictive measurement values (defined as  $Z_{y_{Ni}}$  and  $Z_{y_{ri}}$  respectively) should be the same as the standardized actual measurement value  $Z_{y_i}$ . In other words, when  $n \rightarrow \infty$ ,  $Z_{y_i} = Z_{y_{Ni}} = Z_{y_{ri}}$  all stand for the standardized actual measurement value, but they have different names due to different purposes and various models. Hence,  $Z_{y_{Ni}} \sim N(\mu_{Z_{y_i}}, \sigma_{Z_y}^2)$  and  $Z_{y_{ri}} \sim N(\mu_{Z_{y_i}}, \sigma_{Z_y}^2)$  indicate that  $Z_{y_{Ni}}$  and  $Z_{y_{ri}}$  belong to the same statistical distribution. However, due to different estimating models, the estimations of mean and standard deviation are different between those two prediction algorithms. That is the standardized mean estimating equation ( $\hat{\mu}_{Z_{y_i}} = Z_{\hat{y}_{Ni}}$ ) and standard deviation estimating equation ( $\hat{\sigma}_{Z_y} = \hat{\sigma}_{Z_{y_{Ni}}}$ ) with respect to the NN conjecture model are different from the standardized mean estimating equation ( $\hat{\mu}_{Z_{y_i}} = Z_{\hat{y}_{ri}}$ ) and standard deviation estimating equation ( $\hat{\sigma}_{Z_y} = \hat{\sigma}_{Z_{y_{ri}}}$ ) with respect to the MR reference model.

The purpose of the *RI* is to gauge the reliance level of the virtual measurement value. Therefore, the *RI* should consider degree of similarity between the statistical distribution  $Z_{\hat{y}_{Ni}}$  of the virtual measurement value and the statistical distribution  $Z_{y_i}$  of the actual measurement value. However, when virtual metrology is applied, no actual measurement value is available to verify if the virtual measurement value is trustworthy. (Note that, virtual metrology will not be necessary if actual measurement values are obtained.) Instead, this work adopts the statistical distribution  $Z_{\hat{y}_{ri}}$  estimated by the reference algorithm to replace  $Z_{y_i}$ . Consequently, as indicated in Fig. 2, the *RI* is defined as the intersection-area value (overlap area A) between the statistical distribution  $Z_{\hat{y}_{Ni}}$  of the NN virtual measurement value and the statistical distribution  $Z_{\hat{y}_{ri}}$  of the MR reference prediction value. The *RI* equation is listed below:

$$RI = 2 \int_{\frac{Z_{\hat{y}_{Ni}} + Z_{\hat{y}_{ri}}}{2}}^{\infty} \frac{1}{\sqrt{2\pi}\sigma} e^{-\frac{1}{2}(\frac{x-\mu}{\sigma})^2} dx \quad (4)$$

with  $\mu = Z_{\hat{y}_{Ni}}$  if  $Z_{\hat{y}_{Ni}} < Z_{\hat{y}_{ri}}$

$\mu = Z_{\hat{y}_{ri}}$  if  $Z_{\hat{y}_{ri}} < Z_{\hat{y}_{Ni}}$

and  $\sigma$  is set to be 1.

With larger overlap area A, the *RI* is higher. It indicates that the result from the conjecture model is closer to that of the reference model such that the corresponding virtual measurement value is more reliable. Otherwise, with smaller *RI*, the corresponding virtual measurement value is less reliable. When the distribution  $Z_{\hat{y}_{Ni}}$  estimated from  $Z_{y_{Ni}}$  is totally overlapped with the distribution  $Z_{\hat{y}_{ri}}$  estimated from  $Z_{y_{ri}}$ , according to the distribution theory of statistics, the *RI* value is equal to 1; and, when those two distributions are almost separate, the *RI* value approaches to 0.

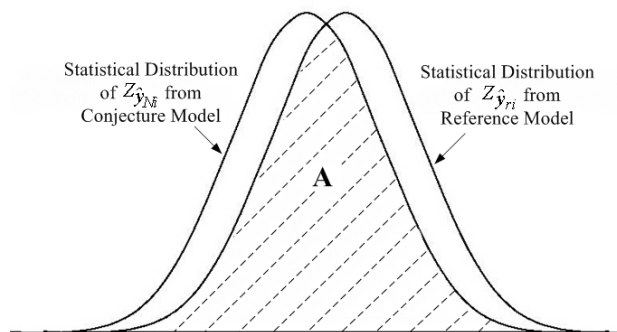


Fig. 2. Statistical Distributions of  $Z_{\hat{y}_{Ni}}$  and  $Z_{\hat{y}_{ri}}$  for Defining the *RI*.

After obtaining the *RI*, the *RI* threshold value ( $RI_T$ ) has to be defined. If  $RI > RI_T$ , then the reliance level of the virtual measurement value is acceptable. A systematic approach for determining the  $RI_T$  is described below.

Before determining the  $RI_T$ , it is necessary to define a maximal tolerable error limit ( $E_L$ ). The error of the virtual measurement value is an absolute percentage of the difference between the actual measurement value  $y_i$  and  $\hat{y}_{Ni}$  obtained from the NN conjecture model divided by the mean of all the actual measurement values,  $\bar{y}$ , namely

$$Error_i = \left| \frac{y_i - \hat{y}_{Ni}}{\bar{y}} \right| \times 100\% \quad (5)$$

The  $E_L$  can then be specified based on the error defined in Eq. (5) and the accuracy specification of VM. Consequently,  $RI_T$  is defined as the *RI* value corresponding to the  $E_L$ , as shown in Fig. 3. That is

$$RI_T = 2 \int_{Z_{Center}}^{\infty} \frac{1}{\sqrt{2\pi}\sigma} e^{-\frac{1}{2}(\frac{x-\mu}{\sigma})^2} dx \quad (6)$$

with  $\mu$  and  $\sigma$  defined in Eq. (4) and

$$Z_{Center} = Z_{\hat{y}_{Ni}} + [\bar{y} \times (E_L / 2)] / \sigma_y \quad (7)$$

where  $\sigma_y$  is specified in Eq. (3).

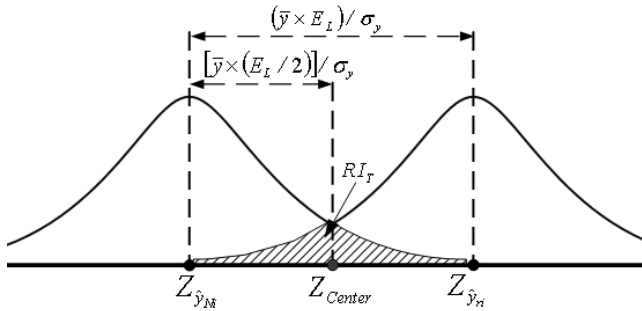


Fig. 3. Statistical Distributions of  $Z_{\hat{y}_N}$  and  $Z_{\hat{y}_t}$  for Defining the  $RI_T$ .

### 2.2 Similarity Indexes (SIs)

As mentioned in Section 2.1, when virtual metrology is applied, no actual measurement value is available to verify if the virtual measurement value is trustworthy. Therefore, instead of the standardized actual measurement value  $Z_{y_i}$ , the standardized MR prediction value  $Z_{\hat{y}_i}$  is adopted to calculate the  $RI$ . This substitution may cause inevitable gauging errors of the  $RI$ . To compensate this unavoidable substitution, the similarity indexes ( $SIs$ ), including a global similarity index ( $GSI$ ) and an individual similarity index ( $ISI$ ), are proposed to assist the  $RI$  in gauging the reliance level of virtual metrology and identifying the key process parameters that have large deviations (z score values).

#### 2.2.1 Global Similarity Index (GSI)

The concept of the  $GSI$  is to evaluate the degree of similarity between a set of process data and the model set of process data. This model set is derived from all of the historical sets of process data used for building the conjecture model.

This work utilizes Mahalanobis distance [5][6] to quantify the degree of similarity. Mahalanobis distance is a distance measure introduced by P.C. Mahalanobis in 1936. It is based on correlation between variables by which different patterns can be identified and analyzed. It is a useful way of determining *similarity* of an unknown sample set to a known one. It differs from Euclidean distance in that it takes into account the correlation of the data set and is scale-invariant, i.e. not dependent on the scale of measurements. If the *similarity* of the data set is high, its Mahalanobis distance calculated will be relatively small.

This work uses the size of the  $GSI$  (i.e. Mahalanobis distance) calculated to discriminate if the set of process data newly entered is similar to the model set of the process data. If the  $GSI$  calculated is small, the newly input set is somewhat similar to the model set. Thus the virtual measurement value conjectured from the newly input (high-similarity) set is relatively accurate. On the contrary, if the  $GSI$  calculated is too large, the newly input set is somewhat different from the model set. Hence the virtual measurement value estimated in accordance with the newly input (low-similarity) set has low reliance level in accuracy.

The equations for computing the standardized process

data  $Z_{x_{i,j}}$  of the conjecture model are shown below:

$$Z_{x_{i,j}} = \frac{x_{i,j} - \bar{x}_j}{\sigma_{x_j}}, i = 1, 2, \dots, n, n+1, \dots, m; j = 1, 2, \dots, p \quad (8)$$

$$\bar{x}_j = \frac{1}{n} (x_{1,j} + x_{2,j} + \dots + x_{n,j}) \quad (9)$$

$$\sigma_{x_j} = \sqrt{\frac{1}{n-1} [(x_{1,j} - \bar{x}_j)^2 + (x_{2,j} - \bar{x}_j)^2 + \dots + (x_{n,j} - \bar{x}_j)^2]} \quad (10)$$

where  $x_{i,j}$  is the  $j$ -th process parameter in the  $i$ -th set of process data,

$Z_{x_{i,j}}$  is the standardized  $j$ -th process parameter in the  $i$ -th set of process data,

$\bar{x}_j$  is the mean of the  $j$ -th process data, and

$\sigma_{x_j}$  is the standard deviation of the  $j$ -th process data.

At first, the model set of the process parameters are defined as  $\mathbf{X}_M = [x_{M,1}, x_{M,2}, \dots, x_{M,p}]^T$ , and let  $x_{M,j}$  equals to  $\bar{x}_j, j = 1, 2, \dots, p$ , so that each element in the model set after standardization (also denoted as the standardized model parameter,  $Z_{M,j}$ ) will all be 0. In other words, all of the elements in  $\mathbf{Z}_M = [Z_{M,1}, Z_{M,2}, \dots, Z_{M,p}]^T$  are 0. Thereafter, the correlation coefficients between the standardized model parameters are calculated.

Assume that the correlation coefficient between the  $s$ -th parameter and the  $t$ -th parameter is  $r_{st}$  and  $k$  sample sets of data are considered, then

$$r_{st} = \frac{1}{k-1} \sum_{l=1}^k z_{sl} \cdot z_{tl} \quad (11)$$

$$= \frac{1}{k-1} (z_{s1} \cdot z_{t1} + z_{s2} \cdot z_{t2} + \dots + z_{sk} \cdot z_{tk})$$

After the correlation coefficients between the standardized model parameters are calculated, the matrix of correlation coefficients can be obtained as:

$$\mathbf{R} = \begin{bmatrix} 1 & r_{12} & \dots & r_{1p} \\ r_{21} & 1 & \dots & r_{2p} \\ \vdots & \vdots & \ddots & \vdots \\ r_{p1} & r_{p2} & \dots & 1 \end{bmatrix} \quad (12)$$

Assume that the inverse matrix ( $\mathbf{R}^{-1}$ ) of  $\mathbf{R}$  is defined as  $\mathbf{A}$ , then

$$\mathbf{A} = \mathbf{R}^{-1} = \begin{bmatrix} a_{11} & a_{12} & \dots & a_{1p} \\ a_{21} & a_{22} & \dots & a_{2p} \\ \dots & \dots & \dots & \dots \\ a_{p1} & a_{p2} & \dots & a_{pp} \end{bmatrix} \quad (13)$$

Hence, the equation for calculating the Mahalanobis distance ( $D_\lambda^2$ ) between the standardized  $\lambda$ -th set process data ( $\mathbf{Z}_\lambda$ ) and the standardized model set process data ( $\mathbf{Z}_M$ ) is listed as follows:

$$D_{\lambda}^2 = (\mathbf{Z}_{\lambda} - \mathbf{Z}_M)^T \mathbf{R}^{-1} (\mathbf{Z}_{\lambda} - \mathbf{Z}_M) = \mathbf{Z}_{\lambda}^T \mathbf{R}^{-1} \mathbf{Z}_{\lambda} \quad (14)$$

Finally, we have

$$D_{\lambda}^2 = \sum_{j=1}^p \sum_{i=1}^p a_{ij} z_{i\lambda} z_{j\lambda} \quad (15)$$

The Mahalanobis distance ( $D_{\lambda}^2$ ) expressed in Eq. (15) is the *GSI* of the standardized  $\lambda$ -th set process data.

After obtaining the *GSI*, the *GSI* threshold ( $GSI_T$ ) should be defined. In general, the default  $GSI_T$  is assigned to be two to three times of the maximal  $GSI_a$  (the subscript “a” stands for each historical set in the training phase).

Further, when the *GSI* corresponding to a certain set of process data is too large, individual similarity indexes (*ISIs*) of all of the parameters in the set have to be analyzed so as to understand which parameter(s) cause this dissimilarity. The explanation for obtaining the *ISIs* of the standardized  $\lambda$ -th set process data,  $Z_{\lambda,j}, j=1, 2, \dots, p$ , are as follows.

### 2.2.2 Individual Similarity Index (ISI)

In fact, the  $\lambda$ -th  $ISI_j, j=1, 2, \dots, p$  are  $Z_{\lambda,j}, j=1, 2, \dots, p$  themselves. If  $Z_{\lambda,j}$  is near zero, this individual parameter is quite similar to the corresponding model parameter  $Z_{M,j} (=0)$ . Therefore, the  $ISI_j$  is defined to be  $Z_{\lambda,j}$  itself and is near zero. On the contrary, if  $Z_{\lambda,j}$  is much larger than three, then  $Z_{\lambda,j}$  is far away from the corresponding standardized model

parameter,  $Z_{M,j}$ . As such, dissimilarity may occur and its corresponding  $ISI_j (=Z_{\lambda,j})$  is much larger than three. A

Pareto chart of *ISIs* can be applied for displaying the dissimilarity tendency. After presenting the algorithms related to the *RI*, *GSI*, and *ISI*, the operating procedures of the VMS is explained below.

### III. VMS OPERATING PROCEDURES

The activity diagram showing the operating procedures of the VMS is depicted in Fig. 4. The operating procedures are divided into the training phase, tuning phase, and conjecturing phase, and each phase contains four parts: NN conjecture, MR reference, *RI*, and *GSI*. Referring to Fig. 1, the NN conjecture part is executed in the conjecture model; the MR reference part and the *RI* part are computed in the *RI* module; and the *GSI* part is calculated in the *SI* module, respectively. The steps for constructing each part in the training phase are presented in the upper portion of Fig. 4.

Production equipment is a time-varying system. Its property will drift or shift as time goes by. Execution of maintenance or part-replacement may also alter the production equipment’s property. To remedy the property-drift problem, the conjecture and reference models should be tuned by a fresh actual measurement sample as shown in the tuning phase of Fig. 4. For example, to accurately conjecture the quality data of 25 pieces of wafers in a semiconductor cassette, at least the quality datum of one wafer in the cassette should be actually measured and served

as the sample for tuning the conjecture and reference models. The tuning phase also has four parts: NN conjecture, MR reference, *RI* and *GSI*. They are described below. After finishing the tuning phase, the conjecturing phase (as shown in the lower portion of Fig. 4) begins.

### IV. IMPLICATIONS OF THE RI AND GSI

After obtaining the  $RI_b$  and  $GSI_b$ , as well as their corresponding  $RI_T$  and  $GSI_T$ , the procedure for determining reliance level of the VMS conjecture result is shown in Fig. 5. If both  $RI_b > RI_T$  and  $GSI_b < GSI_T$  are true, then a green light is on. It indicates that the NN conjecture result and the MR prediction result are quite similar, and the degree of similarity between the set of process data newly entered and the historical sets of process data used for model-building is high, so that great confidence on the virtual measurement value is confirmed.

If  $RI_b > RI_T$  is true and  $GSI_b < GSI_T$  is false, then a blue light is on. It implies that, although the VMS has provided a conjecture result, yet due to the  $GSI_b$  is too high, some

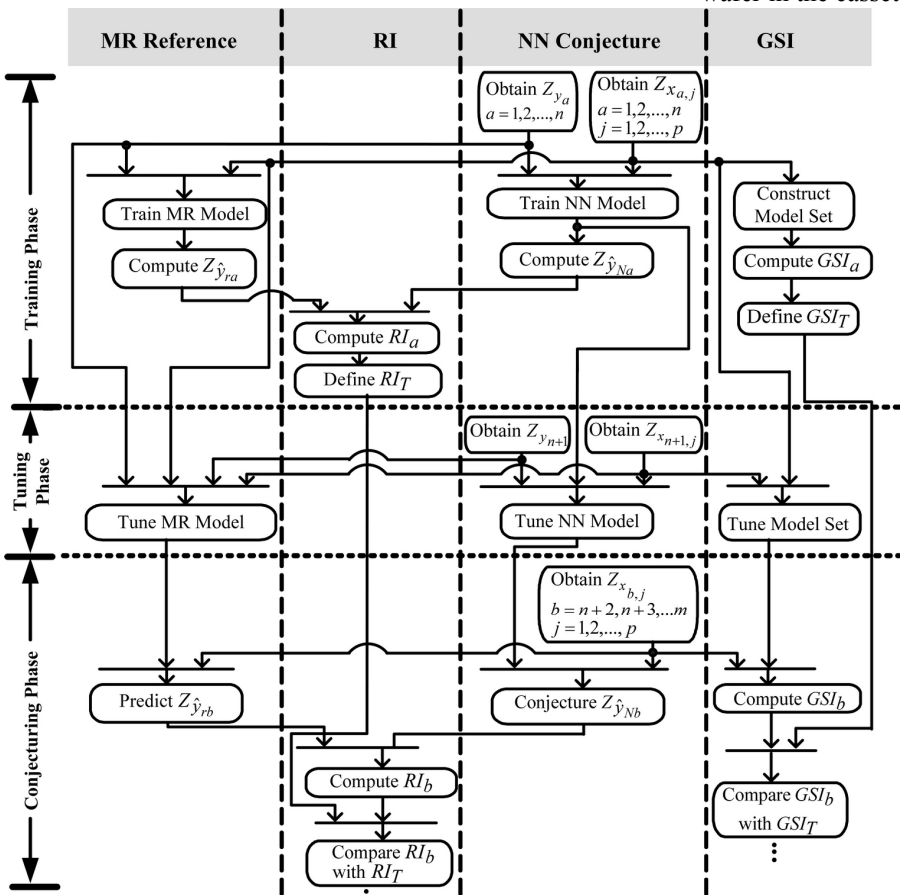


Fig. 4. Operating Procedures of the VMS with the *RI* and *GSI*.

deviations of the process data may occur. Hence, the process data with high  $ISI$  values have to be examined for preventing overconfidence.

If  $RI_b > RI_T$  is false and  $GSI_b < GSI_T$  is true, then a yellow light is on. It means that the virtual measurement value may be inaccurate. However, since the  $GSI_b$  is low, which implies that the degree of similarity (between the set of process data newly entered and the historical sets of process data used for model-building) is high, the situation may be due to bad MR prediction.

If both  $RI_b > RI_T$  and  $GSI_b < GSI_T$  are false, then a red light is on. It infers that large deviation between the NN conjecture result and the MR prediction result occurs. And, since the  $GSI_b$  is too high, the degree of similarity is low. As such, it is confirmed that the virtual measurement value is not reliable. In this case, the most deviant parameter(s) can be identified from the corresponding  $ISI$  Pareto chart. An illustrative example for explaining the applications of the  $RI$ ,  $GSI$ , and  $ISI$  to the VMS is presented as follows.

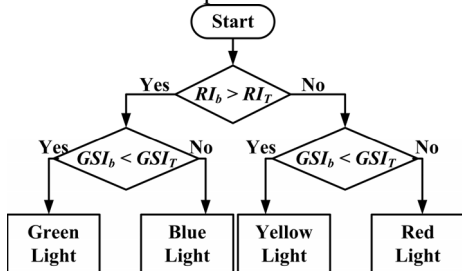


Fig. 5. Flow Chart for Determining Reliance Level of the VMS Conjecture Result.

### V. ILLUSTRATIVE EXAMPLE

This illustrative example is taken from a VMS of production equipment in a 300-mm semiconductor foundry in Taiwan. In this example, there are 125 sets of equipment sample data (process data;  $X_i, i=1, 2, \dots, 125$ ). The 101 sets process data in front have their corresponding actual measurement values ( $y_i, i=1, 2, \dots, 101$ ). It is noted that the 102<sup>th</sup> to 125<sup>th</sup> sets of process data are related to the products currently under manufacturing, hence their actual measurement values ( $y_{102}$  to  $y_{125}$ ) do not exist, and their virtual measurement values are required instead. According to the physical properties of semiconductor equipment and experience of equipment engineers, 24 significant process parameters are selected as the inputs to the NN conjecture model. Among the 125 sets process data and 101 actual measurement values, the first 100 sets of historical process data and 100 historical actual measurement values are used as the training data for building the NN conjecture model. The last 25 (101<sup>th</sup> to 125<sup>th</sup>) sets of process data belong to 25 wafers contained in the same cassette, where the first wafer (101<sup>th</sup>) is usually the sample product whose quality datum is actually measured for the purpose of monitoring the quality of the whole cassette. Consequently, this (101<sup>th</sup>) set of process data and actual measurement value can be used as the data for the tuning purpose. Then, the other 24 (102<sup>th</sup> to 125<sup>th</sup>) sets process data of the cassette are used for performing virtual measurement. As such, in this example,  $n=100; m=125; p=24; a=1, 2, \dots, 100; \text{ and } b=101, 102, \dots, 125$ .

Following the operating procedures shown in Figs. 4 and 5, the results of the illustrative example are presented as

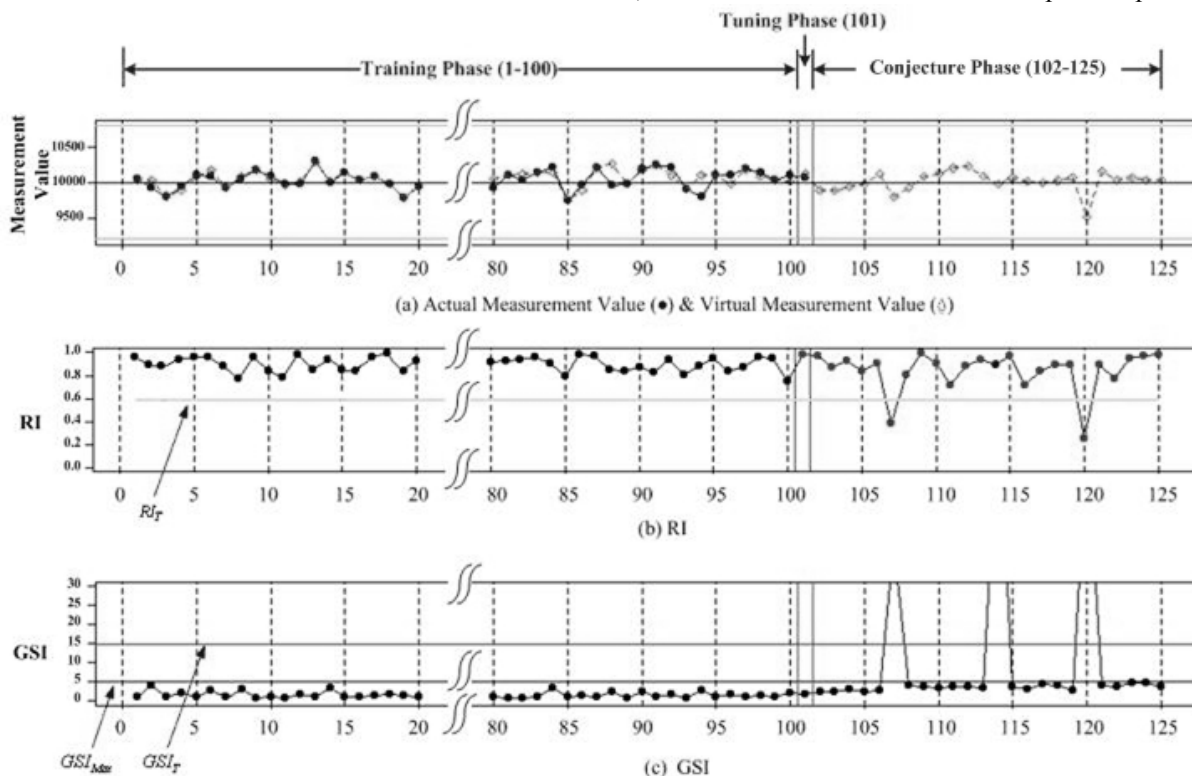


Fig. 6. Real Experimental Results of the Illustrative Example.

follows. The actual and virtual measurement values,  $RI$  values, and  $GSI$  values in the training, tuning, and conjecturing phases are shown in Figs. 6(a), 6(b), and 6(c), respectively.

In the training phase ( $a=1, 2, \dots, 100$ ), both the actual and virtual measurement values are shown in Fig. 6(a). The  $RI_a$  and  $GSI_a$  are displayed in Figs. 6(b) and 6(c), respectively. The  $RI_T (=0.567)$  is obtained with the specified  $E_L$  (3%) and is depicted in Fig. 6(b). The  $GSI_{Max}$  during the training phase is about 5, so the  $GSI_T$  is assigned to be 15. Both the  $GSI_{Max}$  and  $GSI_T$  are shown in Fig. 6(c). During the tuning phase ( $b=101$ ), both the actual and virtual measurement values,  $RI_{101}$ , and  $GSI_{101}$  are shown in Fig. 6(a), 6(b), and 6(c), respectively. As for the conjecturing phase ( $b=102, 103, \dots, 125$ ), only the virtual measurement values,  $RI_b$ , and  $GSI_b$  are presented in Fig. 6(a), 6(b), and 6(c), respectively.

Observing the 107<sup>th</sup> and 120<sup>th</sup> data sets, since their  $RI$ s are smaller than the  $RI_T$ , it indicates that there is no confidence on the virtual measurement values  $\hat{y}_{N_{107}}$  and  $\hat{y}_{N_{120}}$ . Moreover, since their  $GSI$ s are greater than the  $GSI_T$ , bad reliance level of  $\hat{y}_{N_{107}}$  and  $\hat{y}_{N_{120}}$  are confirmed. Therefore, red lights are shown on  $RI_{107}$  and  $RI_{120}$ . In these cases, their associated  $ISIs$  of the 107<sup>th</sup> and 120<sup>th</sup> sets process data have to be checked to understand whose process data are deviated from the historical sets process data for model-building, thereby locating the problems.

Referring to the 114<sup>th</sup> data set, since its  $RI_{114}$  is greater than the  $RI_T$  but its  $GSI_{114}$  is greater than the  $GSI_T$ , it implies that the corresponding  $ISIs$  of the 114<sup>th</sup> set process data have to be checked for preventing overconfidence on the reliance level. The blue light is shown on  $RI_{114}$  for this case.

Except for the 107<sup>th</sup>, 114<sup>th</sup>, and 120<sup>th</sup> data sets, since the  $RI$ s of the remaining data sets are greater than the  $RI_T$ , and their corresponding  $GSI$ s are smaller than the  $GSI_T$ , it concludes that their corresponding virtual measurement values  $\hat{y}_{N_b}$  are all reliant. As such, the green lights are shown on all of the corresponding  $RI_b$ .

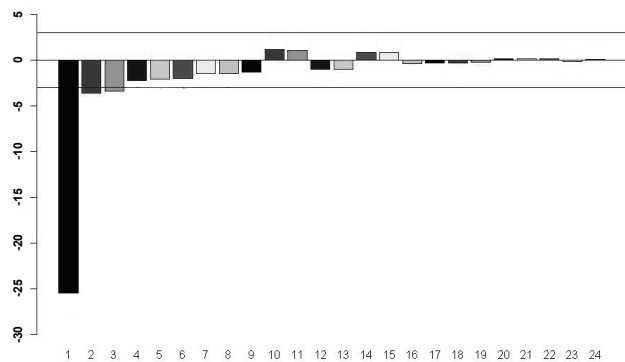


Fig. 7. ISI Pareto Chart of the 107<sup>th</sup> Set Process Data.

When  $GSI_b > GSI_T$  occurs, the corresponding  $ISIs$  of the process data shall be examined such that the cause of deviation may be identified. Taking the 107<sup>th</sup> data set as an

example and referring to Fig. 7, it can be found that the 13<sup>th</sup> parameter in the  $ISI$  Pareto chart has the largest deviation.

## VI. SUMMARY AND CONCLUSIONS

A method for evaluating reliance level of a virtual metrology system is proposed. In this method, a reliance index ( $RI$ ) and a  $RI$  threshold ( $RI_T$ ) value are calculated by analyzing the process data of production equipment, thereby determining if the virtual metrology result is reliant. In addition, a global similarity index ( $GSI$ ) and an individual similarity index ( $ISI$ ) are also proposed for defining the degree of similarity between the input set process data and all of the historical sets process data used for establishing the conjecture model, thereby assisting in gauging the degree of reliance. Based on the results of the illustrated example, this proposed method with the  $RI$ ,  $GSI$ , and  $ISI$  is believed to be feasible and can make the VMS manufacturable.

## REFERENCES

- [1] J. Chang and F.-T. Cheng, "Application Development of Virtual Metrology in Semiconductor Industry," in *Proc. of The 31th Annual Conference of the IEEE Industrial Electronics Society (IECON 2005)*, Raleigh, North Carolina, U.S.A., pp. 124-129, November 2005.
- [2] Y.-C. Su, M.-H. Hung, F.-T. Cheng, and Y.-T. Chen, "A Processing Quality Prognostics Scheme for Plasma Sputtering in TFT-LCD Manufacturing," *IEEE Transactions on Semiconductor Manufacturing*, vol. 19, no. 2, pp. 183-194, May 2006.
- [3] Y.-C. Su, F.-T. Cheng, M.-H. Hung, and H.-C. Huang, "Intelligent Prognostics System Design and Implementation," *IEEE Transactions on Semiconductor Manufacturing*, vol. 19, no. 2, pp. 195-207, May 2006.
- [4] R. L. Mason, R. F. Gunst, and J. L. Hess, *Statistical Design and Analysis of Experiments with Applications to Engineering and Science*, New York: Wiley, 1989.
- [5] G. Taguchi, S. Chowdhury, and Y. Wu, *The Mahalanobis-Taguchi System*, New York: McGraw-Hill, 2001.
- [6] G. Taguchi, and R. Jugulum, *The Mahalanobis-Taguchi Strategy: A Pattern Technology System*, New York: McGraw-Hill, 2002.
- [7] T.-H. Lin, M.-H. Hung, R.-C. Lin, and F.-T. Cheng, "A Virtual Metrology Scheme for Predicting CVD Thickness in Semiconductor Manufacturing," in *Proc. 2006 IEEE International Conference on Robotics and Automation*, Orlando, Florida, U.S.A., pp.1054-1059, May 2006.
- [8] Y.-T. Huang, F.-T. Cheng, and Y.-T. Chen, "Importance of Data Quality in Virtual Metrology," to appear in *Proc. of The 32th Annual Conference of the IEEE Industrial Electronics Society (IECON 2006)*, Paris, France, November 2006.
- [9] J. Chang and F.-T. Cheng, "Manufacturability of Multivariate Applications in the Semiconductor Industry," to appear in *Proc. 2006 IEEE International Conference on Automation Science and Engineering*, Shanghai, China, October 2006.